

## Texture analysis in cone-beam computed tomographic images of medication-related osteonecrosis of the jaw

Polyane Mazucatto Queiroz<sup>1,2,\*</sup>, Karolina Castilho Fardim<sup>2</sup>, André Luiz Ferreira Costa<sup>3</sup>, Ricardo Alves Matheus<sup>4</sup>, Sérgio Lúcio Pereira Castro Lopes<sup>2</sup>

<sup>1</sup>Department of Dentistry, Ingá University Center, Maringá, Brazil

<sup>2</sup>Department of Diagnosis and Surgery, São José dos Campos School of Dentistry, São Paulo State University, São José dos Campos, Brazil

<sup>3</sup>Postgraduate Program in Dentistry, Cruzeiro do Sul University, São Paulo, Brazil

<sup>4</sup>Department of Oral Medicine, State University of Londrina, Londrina, Brazil

### ABSTRACT

**Purpose:** The aim of this study was to evaluate changes in the trabecular bone through texture analysis and compare the texture analysis characteristics of different areas in patients with medication-related osteonecrosis of the jaw (MRONJ).

**Materials and Methods:** Cone-beam computed tomographic images of 16 patients diagnosed with MRONJ were used. In sagittal images, 3 regions were chosen: active osteonecrosis (AO); intermediate tissue (IT), which presented a zone of apparently healthy tissue adjacent to the AO area; and healthy bone tissue (HT) (control area). Texture analysis was performed evaluating 7 parameters: secondary angular momentum, contrast, correlation, sum of squares, inverse moment of difference, sum of entropies, and entropy. Data were analyzed using the Kruskal-Wallis test with a significance level of 5%.

**Results:** Comparing the areas of AO, IT, and HT, significant differences ( $P < 0.05$ ) were observed. The IT and AO area images showed higher values for parameters such as contrast, entropy, and secondary angular momentum than the HT area, indicating greater disorder in these tissues.

**Conclusion:** Through texture analysis, changes in the bone pattern could be observed in areas of osteonecrosis. The texture analysis demonstrated that areas visually identified and classified as IT still had necrotic tissue, thereby increasing the accuracy of delimiting the real extension of MRONJ. (*Imaging Sci Dent* 2023; 53: 109-15)

**KEY WORDS:** Diagnostic Imaging; Bisphosphonate-Associated Osteonecrosis of the Jaw; Cone-Beam Computed Tomography; Image Processing, Computer-Assisted

### Introduction

Antiresorptive and antiangiogenic drugs are successfully used to treat different changes in bone metabolism, from osteopenia to metastases of malignant neoplasms in bone tissues. Antiresorptive drugs can compromise the activity of osteoclasts, inhibiting the process of bone resorption and remodeling. Antiangiogenic drugs decrease angiogenesis,

which reduces the vascular supply of bone tissue.<sup>1-3</sup> The changes in bone metabolism resulting from these medications can trigger bone necrosis as a side effect.

Although any bone tissue is subject to this side effect, the presence of trauma can promote the manifestation of osteonecrosis. Trauma resulting from surgical interventions, such as the extraction and installation of implants, or due to constant trauma to the jaws from poorly adapted prostheses or even the patient's own occlusion, is a risk factor.<sup>2-4</sup> The presence of a risk factor increases the chance of manifestation of necrosis in the jaws of patients who use antiresorptive and antiangiogenic medications, which is an inflammatory condition known as medication-related osteonecro-

Received November 22, 2022; Revised December 26, 2022; Accepted January 14, 2023  
Published online February 11, 2023

\*Correspondence to : Prof. Polyane Mazucatto Queiroz  
Department of Dentistry, Ingá University Center, 6114 Rod PR 317, Maringá 87035-510, Parana, Brazil  
Tel) 55-44-3033-5009, E-mail) polyanequeiroz@hotmail.com

Copyright © 2023 by Korean Academy of Oral and Maxillofacial Radiology

This is an Open Access article distributed under the terms of the Creative Commons Attribution Non-Commercial License (<http://creativecommons.org/licenses/by-nc/3.0>) which permits unrestricted non-commercial use, distribution, and reproduction in any medium, provided the original work is properly cited.

Imaging Science in Dentistry · pISSN 2233-7822 eISSN 2233-7830

sis of the jaw (MRONJ). This condition mainly presents in women, and the most frequently affected site is the posterior region of the mandible.<sup>1,3,4</sup>

Clinically, patients may present with purulent secretion, edema, and/or the presence of an intraoral or extraoral fistula, or may even be asymptomatic.<sup>1,2,5</sup> On radiographic examinations, a radiolucent area with irregular borders is observed, with an aspect of bone destruction.<sup>6</sup> In a 3-dimensional visualization using cone-beam computed tomography (CBCT) images, it is possible to evaluate the bone tissue without overlap, helping to identify compromised areas that would not be visualized on conventional radiographs.<sup>7-10</sup>

With the additional information obtained from CBCT images, it is possible to determine a more adequate treatment plan considering the actual extent of the lesion.<sup>5,7-9,11</sup> However, while CBCT images can be obtained with gray-scales up to 16 bits in depth (65,536 shades of gray), the human eye has a limited capacity to identify approximately only 60 shades of gray,<sup>12</sup> such that variations in the bone pattern present in the image may not be identified with the naked eye. This factor may hinder a reliable delimitation of the area affected by MRONJ or even underestimate the extent of the lesion.

Thus, an objective analysis of tomographic images must be considered. These images present characteristics, such as smoothness, graininess, roughness, and homogeneity, which are determined by the shades of gray represented in the image.<sup>13-15</sup> These image features can be identified from texture analysis.

Texture analysis is a mathematical method of evaluating gray tones and the relationship/distribution between adjacent gray tones that can help characterize the tissue under study.<sup>15,16</sup> Texture analysis has been successfully used in the medical field to evaluate changes in ischemic stroke,<sup>13</sup> osteoarthritis,<sup>17</sup> osteoporosis,<sup>18</sup> and intraosseous lipoma.<sup>19</sup> As well, in dentistry, it has already been used to evaluate periodontal alterations in the furcation region,<sup>20</sup> oral cancer,<sup>21</sup> bone grafts used in maxillary sinus lift surgery,<sup>22</sup> and dental implant stability.<sup>23</sup> However, a more detailed and accurate assessment of the bone pattern in cases of MRONJ in the mandible was not identified in the reviewed literature.

Considering the possibility of pointing out changes in tomographic images not identified by the human eye, it is necessary to evaluate the applicability of texture analysis as a tool for detecting osteonecrosis even in regions diagnosed by the human eye as healthy tissue. Thus, the present study was developed with the objective of evaluating the ability of texture analysis to detect changes in the trabecular bone and comparing the texture analysis characteristics of different

areas in patients with MRONJ. The hypothesis was that there would be statistically significant differences in texture analysis parameters of areas of active osteonecrosis, intermediate tissue around the lesion, and healthy bone tissue.

## Materials and Methods

The present study is experimental, analytical, and diagnostic research carried out at the Radiology Clinic of the Department of Diagnosis and Surgery of São José dos Campos School of Dentistry. At the time of each examination, the patient's authorization was requested for the use of the image in research through an informed consent form. The proposed project was approved by the Ethics Committee via Plataforma Brasil under number 40680920.2.0000.5220.

### Sample

CBCT images of 16 patients aged 56 to 82 years (mean age, 71 years) who were on continuous use of antiresorptive medication (bisphosphonate) who were diagnosed with MRONJ were selected. The inclusion criteria were examinations that showed visible mandibular alterations and presented a confirmed clinical and radiographic diagnosis of MRONJ. Examinations in which the field of view did not register the entire mandible and those with movement artifacts that made it impossible to see the region clearly were excluded. All images were obtained on the OP 3D Vision tomograph (Imaging Science International, Hatfield, PA, USA) with 5 mA, 120 kVp, 7.42 s, 0.20 mm voxel size, and an 8 cm × 8 cm field of view, covering the entire mandible. The images were obtained in the Digital Imaging and Communications in Medicine (DICOM) format.

### Image analysis

All images were exported in DICOM format to On-Demand3D software version 1.0 (Cybermed Inc., Seoul, Korea). In this software, the examination was visualized in the "Dental Module." In the multiplanar reconstruction window, 2 dentomaxillofacial radiologists with more than 10 years of experience in CBCT imaging selected, by consensus, 2 sagittal images of each volume with a section thickness of 0.20 mm: 1 image of the bone necrosis area and 1 sagittal image of the opposite side, in the region of healthy tissue.

Rectangular regions of interest (ROIs) with dimensions of 25 × 10 pixels were delimited using the ROI tool in 3 regions: regions with a tomographic appearance of active osteonecrosis (AO), regions with a tomographic appearance of intermediate tissue (IT) (aspect of healthy tissue adjacent to

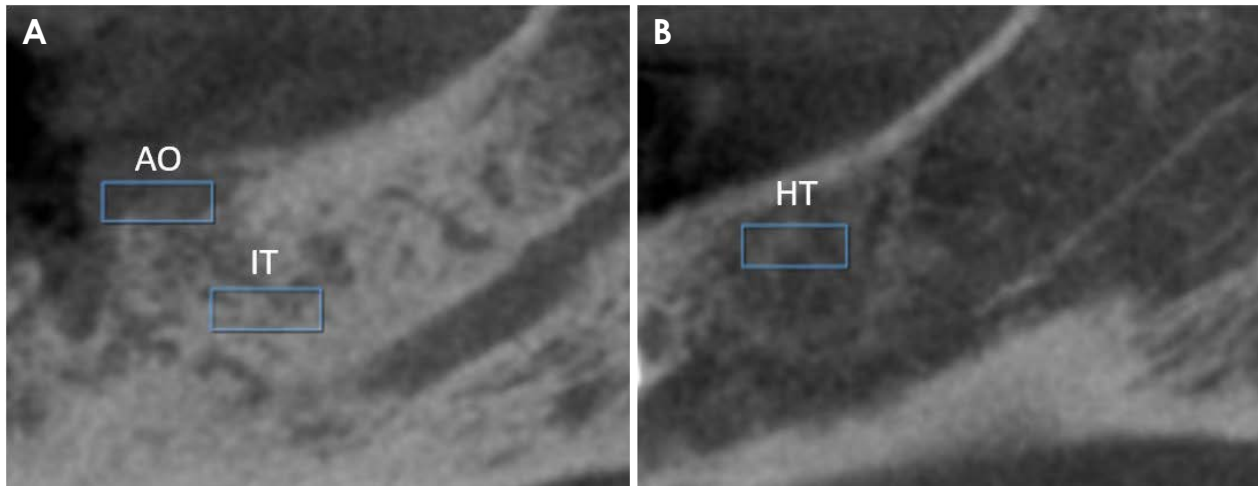


**Fig. 1.** A. Sagittal image of the osteonecrosis region, where AO is the region with a tomographic appearance of active osteonecrosis and IT is the region with a tomographic appearance of intermediate tissue (the aspect of healthy tissue adjacent to the area of necrosis). B. Sagittal image of the side opposite to osteonecrosis, with HT being the region with a tomographic appearance of healthy bone tissue.

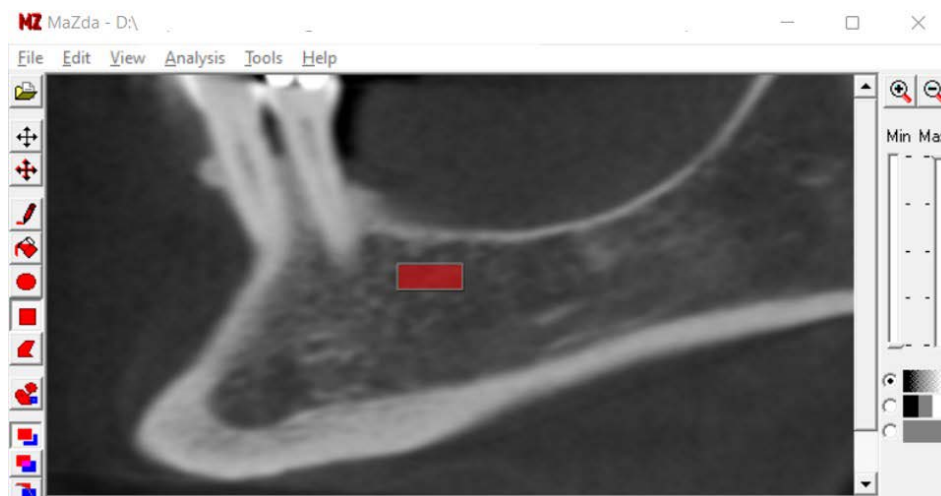


**Fig. 2.** A region of interest is delimited in the MaZda software to perform texture analysis.

the area of necrosis), and regions with a tomographic appearance of healthy bone tissue (HT) as the control area. Subsequently, the images were saved in the bitmap format (.bmp), individually, with the ROI marked so that the AO could be visualized in the delimited regions (Fig. 1).

### Texture analysis

A dentomaxillofacial radiologist performed texture analysis using MaZda 3.20 software (Institute of Electronics, Technical University of Lodz, Poland) by a dental radiologist with more than 10 years of experience. In this software, the “Draw Polygon” tool was used to delimit the ROI (Fig. 2) previously determined in OnDemand3D.

Texture analysis was performed using a statistical approach through gray-level co-occurrence matrix (GLCM) anal-

ysis. This study evaluated 7 texture analysis factors used in the study by Costa et al.<sup>23</sup> 1) angular second moment (a measurement of image uniformity), 2) contrast (representing the variation in shades of gray), 3) correlation (a measurement dependent on grayscales between neighboring pixels), 4) sum of squares (a measurement of grayscale dispersion), 5) inverse difference moment (an indicator of the homogeneity of shades of gray), 6) sum of entropies (the sum of the disorganization of the distribution of shades of gray), and 7) entropy (the degree of disorder between pixels).

The texture parameters related to GLCM analysis were first selected in the “Analysis Option” window. To evaluate the shades of gray in different positions, in the “Maps” tab, matrix parameters were selected in relation to the direction of the pixels: horizontal (0°), vertical (90°), and angles of

**Table 1.** Mean and standard deviation of the values of the factors studied in the regions of active osteonecrosis, intermediate tissue, and healthy tissue

	Active osteonecrosis	Intermediate tissue	Healthy tissue	<i>P</i> -value
Angular second moment	0.031 ( $\pm 0.02$ ) <sup>A</sup>	0.021 ( $\pm 0.02$ ) <sup>B</sup>	0.049 ( $\pm 0.05$ ) <sup>C</sup>	<0.05
Contrast	7.787 ( $\pm 7.78$ ) <sup>A</sup>	9.375 ( $\pm 9.54$ ) <sup>B</sup>	5.446 ( $\pm 5.75$ ) <sup>C</sup>	<0.05
Correlation	0.715 ( $\pm 0.23$ ) <sup>A</sup>	0.736 ( $\pm 0.22$ ) <sup>A</sup>	0.525 ( $\pm 0.32$ ) <sup>B</sup>	<0.05
Sum of squares	14.996 ( $\pm 7.95$ ) <sup>A</sup>	22.751 ( $\pm 14.67$ ) <sup>B</sup>	6.335 ( $\pm 4.64$ ) <sup>C</sup>	<0.05
Inverse difference moment	0.470 ( $\pm 0.16$ ) <sup>A</sup>	0.435 ( $\pm 0.15$ ) <sup>B</sup>	0.514 ( $\pm 0.17$ ) <sup>C</sup>	<0.05
Sum of entropy	1.333 ( $\pm 0.13$ ) <sup>A</sup>	1.404 ( $\pm 0.14$ ) <sup>B</sup>	1.131 ( $\pm 0.17$ ) <sup>C</sup>	<0.05
Entropy	1.846 ( $\pm 0.27$ ) <sup>A</sup>	1.943 ( $\pm 0.24$ ) <sup>B</sup>	1.609 ( $\pm 0.33$ ) <sup>C</sup>	<0.05

\*Different letters on the same line indicate a significant difference between regions for the corresponding factor, considering a significance level of 5%.

45° and 135°. The values referring to each factor studied were tabulated for each study area.

### Statistical analysis

The tabulated data were analyzed using the BioEstat software (Fundação Mamirauá, Belém, Brazil). The Shapiro-Wilk normality test was performed. The data did not show a normal distribution, so for each factor, the 3 areas (affected, intermediate, and healthy) were compared using the Kruskal-Wallis test with the *post-hoc* Student-Newman-Keuls test, considering a significance level of 5% ( $P < 0.05$ ).

### Results

The patients had a mean age of 67 years; the majority (68.75%) were women and 31.25% were men. Comparing the areas of AO, IT, and HT, significant differences ( $P < 0.05$ ) were observed for all factors studied, as shown in Table 1.

A significant difference ( $P < 0.05$ ) was observed between the angular second moment values of the 3 studied areas, with a higher value in the healthy area.

For contrast, a significant difference ( $P < 0.05$ ) was observed among the 3 studied areas, with a lower value in the healthy area and a higher value in the intermediate area.

A significant difference ( $P < 0.05$ ) was observed in the correlation values of the 3 studied areas. However, no significant difference was observed between the area with active osteonecrosis and the intermediate area ( $P = 0.255$ ), which presented higher values than the healthy area.

For the sum of squares, a significant difference ( $P < 0.05$ ) was observed among the 3 studied areas, with a lower value in the healthy area and a higher value in the intermediate area.

A significant difference ( $P < 0.05$ ) was observed in the

values of the inverse difference moment of the 3 studied areas, with a higher value in the healthy area and a lower value in the intermediate area.

A significant difference was observed in the sum of entropy values ( $P < 0.05$ ) and entropy values ( $P < 0.05$ ) among the 3 studied areas, with lower values in the healthy area and higher values in the intermediate area.

### Discussion

MRONJ is a low-incidence condition, but it causes unpleasant symptoms and can result in important complications, such as fistulas, extensive infectious processes, and bone fractures. The treatment of MRONJ is associated with the stage of development of the condition, which is classified based on clinical characteristics and imaging tests.<sup>2,3,10</sup>

In radiographic images, some important aspects can be observed in patients with MRONJ, such as areas of osteolysis, changes in the trabecular bone pattern, bone loss, dense bone, non-repair of bone in the post-surgical area, and bone sequestration.<sup>6,10</sup> Considering the inherent limitations of radiographic images, tomographic images can be used to better assess the characteristics associated with the severity and extent of the lesion.<sup>10,24</sup> Although, in general, bone changes can be visualized on CBCT images, small structural variations that are not visually perceptible may occur.<sup>20</sup> In addition, CBCT presents information relevant for the interpretation of tissue characteristics that are associated with image pixel distribution. These characteristics can be studied through texture analysis.<sup>17</sup>

Texture analysis provides an objective and quantitative assessment of the distribution and relationship between the grayscale values of an image. The most frequently applied method is GLCM analysis, which considers the repetition (co-occurrence) of shades of gray at a distance  $d$  and with an

angle  $\times$  for different directions. Normally, the  $0^\circ$ ,  $45^\circ$ ,  $90^\circ$ , and  $135^\circ$  angles are the most used.<sup>20</sup> Thus, in the present study, the MaZda software was used for the interpretation of texture analysis by GLCM in these usual directions. The MaZda software has already been used in clinical studies to evaluate bone loss detection in the furcation region,<sup>20</sup> bone grafts performed for maxillary sinus lift procedures,<sup>22</sup> and cerebrovascular accidents.<sup>13</sup> This software has been presented as one of the most appropriate for texture analysis.<sup>14</sup>

Texture analysis is a resource that can be used to evaluate images by characterizing bone microarchitecture, which shows a close correlation with the histomorphometric patterns of bone tissue.<sup>22,25</sup> This method of detailed analysis incorporates information beyond the human visual capacity; this makes texture analysis an important tool because some apparently healthy areas may contain altered bone tissue not detected by the human eye.<sup>20</sup>

Considering the importance of characterizing tissue with MRONJ and determining the correct extent of osteonecrosis in the tissue to select a treatment plan, this detailed analysis may provide useful information for diagnosis and planning. In the present study, the value of the moment of inverse difference was lower in the intermediate areas, indicating less homogeneity than in other regions.<sup>15,16</sup> This can be confirmed by the greater contrast in the intermediate region, indicating greater noise and lack of uniformity. Instead, the healthy area presented an inverse moment of difference and contrast compatible with a more uniformly patterned tissue, providing evidence for a difference in the bone pattern between the healthy area and the intermediate area.

This apparently healthy intermediate area showed a very significant pattern of disorganization, as expressed by the high values of sum of squares, sum entropy and entropy. These 3 factors are correlated with the distribution of variance, mean dispersion, and degree of disorder, respectively.<sup>15,16</sup> This tissue disorganization, even greater than that observed in tissue with active osteonecrosis, may be due to the fact that necrotic tissue and healthy tissue may be present in this intermediate area, mixing these 2 patterns.

This similarity between the intermediate area and the tissue with active osteonecrosis was also supported by the statistical study of the relationship between pixels. The correlation factor measures the linear dependence between neighboring pixels.<sup>15,16</sup> In the present study, a lower dependence was observed between pixels in the healthy tissue in relation to the affected and intermediate tissues, which showed no difference between them. A likely explanation for this is that healthy tissue shows a texture of bone trabeculae and medullary spaces that are independent. In tissues

where there is osteonecrosis, there is a change in the bone pattern.<sup>6,10</sup> Thus, in tissues with active and intermediate osteonecrosis, there is a greater dependence between pixels, since there is a similar pattern of disorganization in this tissue, without the difference in the characteristics of medullary trabeculae and bone spaces. This factor reinforces the change in the pattern of tissue with necrosis, and the finding that the apparently healthy intermediate tissue presented the same pattern of correlation as the tissue with active osteonecrosis confirms the importance of these characteristics for the correct definition of the limits of the areas of tissue osteonecrosis. Considering the difficulty in treating MRONJ,<sup>10</sup> a correct delimitation of the affected area by texture analysis will probably increase the assertiveness of the plan of treatment.<sup>20</sup>

As shown in Table 1, the regions related to the intermediate bone presented the highest values for 5 of the 7 parameters analyzed: contrast, correlation, sum of squares, sum of entropy, and entropy. The regions of affected bone presented the second-highest values of the same parameters. For these, the healthy bone regions had the lowest values. High values for these parameters, such as contrast, entropy, sum of entropy, sum of squares and angular second moment, point to a greater disorder and lack of uniformity in the distribution of image pixels, indicating regions affected by osteolytic processes. This finding indicates that, even if the intermediate regions were classified as unaffected areas through a visual inspection of the images, resorption processes were already taking place in those areas. That is, bone visually classified as borderline healthy/unaffected can already show altered behavior involving MRONJ.

These findings can greatly influence the planning process in the delimitation of the lesion and establishment of the dimensions of the affected region of necrotic bone; furthermore, these results also explain the frequent occurrence that, during surgical intervention procedures for curettage of MRONJ regions, the region is discovered to be in fact much larger than seen on imaging.

As for the parameters that indicate greater uniformity and balance - angular second moment and inverse difference moment<sup>16</sup> - the healthy bone regions had the highest values of the groups, indicating the uniformity and standardization of the distribution of gray levels in the image. It is noted that for these 2 parameters, the regions of intermediate bone presented the lowest mean values, lower even in relation to those of regions affected by MRONJ. This indicates that the behavior of the intermediate regions emphatically differed from that observed for healthy regions, further emphasizing that these areas are not regions that can be considered

healthy and capable of maintenance in cases of curettage.

Considering the meticulousness of the information obtained through texture analysis, future studies could be conducted in order to assess the possibility of early diagnosis of osteonecrosis. This indication is already applied by neurologists for the early diagnosis of ischemic stroke and for quantifying the real extent of the entire affected area.<sup>13</sup>

Thus, evidence was found that texture analysis technique made it possible to evaluate the real bone involvement of border regions between areas evidently affected by MRONJ and healthy areas, thereby providing valuable information and underscoring the need for an objective process to be used in image analysis for delimiting lesions and surgical planning.

It is important to emphasize that this study is pioneering and needs further development, such as a study with a larger sample and the possibility of cross-referencing the CBCT observations and the actual surgical findings, but it is evident that texture analysis can be considered as a promising complementary method for this goal.

Through texture analysis, it was possible to observe changes in the trabecular bone pattern in areas affected by osteonecrosis. In addition, texture analysis made it possible to visually identify that areas classified as intermediate areas had necrotic tissue, thus increasing the accuracy of delimiting the real extension of MRONJ.

**Conflicts of Interest:** None

## References

- Lorenzo-Pouso AI, Bagán J, Bagán L, Gándara-Vila P, Chamorro-Petronacci CM, Castelo-Baz P, et al. Medication-related osteonecrosis of the jaw: a critical narrative review. *J Clin Med* 2021; 10: 4367.
- Yarom N, Shapiro CL, Peterson DE, Van Poznak CH, Bohlke K, Ruggiero SL, et al. Medication-related osteonecrosis of the jaw: MASCC/ISOO/ASCO clinical practice guideline. *J Clin Oncol* 2019; 37: 2270-90.
- Alsalihi A, Dam A, Lindberg P, Truedsson A. Medication-related osteonecrosis of the jaws initiated by zoledronic acid and potential pathophysiology. *Dent J (Basel)* 2021; 9: 85.
- Singh M, Gonegandla GS. Bisphosphonate-induced osteonecrosis of the jaws (BIONJ). *J Maxillofac Oral Surg* 2020; 19: 162-7.
- Eguia A, Bagán-Debón L, Cardona F. Review and update on drugs related to the development of osteonecrosis of the jaw. *Med Oral Patol Oral Cir Bucal* 2020; 25: e71-83.
- Kawahara M, Kuroshima S, Sawase T. Clinical considerations for medication-related osteonecrosis of the jaw: a comprehensive literature review. *Int J Implant Dent* 2021; 7: 47.
- Baba A, Goto TK, Ojiri H, Takagiwa M, Hiraga C, Okamura M, et al. CT imaging features of antiresorptive agent-related osteonecrosis of the jaw/medication-related osteonecrosis of the jaw. *Dentomaxillofac Radiol* 2018; 47: 20170323.
- Shin WJ, Kim CH. Prognostic factors for outcome of surgical treatment in medication-related osteonecrosis of the jaw. *J Korean Assoc Oral Maxillofac Surg* 2018; 44: 174-81.
- Pichardo SE, Broek FW, Fiocco M, Appelman-Dijkstra NM, van Merkesteyn JP. A comparison of the cone beam computed tomography findings in medication-related osteonecrosis of the jaws related to denosumab versus bisphosphonates: an observational pilot study. *Oral Surg Oral Med Oral Pathol Oral Radiol* 2020; 129: 411-7.
- Kün-Darbois JD, Fauvel F. Medication-related osteonecrosis and osteoradionecrosis of the jaws: update and current management. *Morphologie* 2021; 105: 170-87.
- Huber FA, Schumann P, von Spiczak J, Wurnig MC, Klarhöfer M, Finkenstaedt T, et al. Medication-related osteonecrosis of the jaw-comparison of bone imaging using ultrashort echo-time magnetic resonance imaging and cone-beam computed tomography. *Invest Radiol* 2020; 55: 160-7.
- Voigt H. The 'digital eye' at the threshold of cancer diagnosis. *Expert Rev Anticancer Ther* 2002; 2: 479-80.
- Oliveira MS, Fernandes PT, Avelar WM, Santos SL, Castellano G, Li LM. Texture analysis of computed tomography images of acute ischemic stroke patients. *Braz J Med Biol Res* 2009; 42: 1076-9.
- Szczypiński PM, Strzelecki M, Materka A, Klepaczko A. MaZda - a software package for image texture analysis. *Comput Methods Programs Biomed* 2009; 94: 66-76.
- Lubner MG, Smith AD, Sandrasegaran K, Sahani DV, Pickhardt PJ. CT texture analysis: definitions, applications, biologic correlates, and challenges. *Radiographics* 2017; 37: 1483-503.
- Haralick RM, Shanmugam K, Dinstein I. Textural features for image classification. *IEEE Trans Syst Man Cybern* 1973; 3: 610-21.
- Hirvasniemi J, Gielis WP, Arbabi S, Agricola R, van Spil WE, Arbabi V, et al. Bone texture analysis for prediction of incident radiographic hip osteoarthritis using machine learning: data from the Cohort Hip and Cohort Knee (CHECK) study. *Osteoarthritis Cartilage* 2019; 27: 906-14.
- Kavitha MS, An SY, An CH, Huh KH, Yi WJ, Heo MS, et al. Texture analysis of mandibular cortical bone on digital dental panoramic radiographs for the diagnosis of osteoporosis in Korean women. *Oral Surg Oral Med Oral Pathol Oral Radiol* 2015; 119: 346-56.
- Lee KM, Kim HG, Lee YH, Kim EJ. mDixon-based texture analysis of an intraosseous lipoma: a case report and current review for the dental clinician. *Oral Surg Oral Med Oral Pathol Oral Radiol* 2018; 125: e67-71.
- Gonçalves BC, de Araújo EC, Nussi AD, Bechara N, Sarmiento D, Oliveira MS, et al. Texture analysis of cone-beam computed tomography images assists the detection of furcal lesion. *J Periodontol* 2020; 91: 1159-66.
- Raja JV, Khan M, Ramachandra VK, Al-Kadi O. Texture analysis of CT images in the characterization of oral cancers involving buccal mucosa. *Dentomaxillofac Radiol* 2012; 41: 475-80.
- Marchand-Libouban H, Guillaume B, Bellaiche N, Chappard D. Texture analysis of computed tomographic images in osteoporotic patients with sinus lift bone graft reconstruction. *Clin Oral*

- Investig 2013; 17: 1267-72.
23. Costa AL, de Souza Carreira B, Fardim KA, Nussi AD, da Silva Lima VC, Miguel MM, et al. Texture analysis of cone beam computed tomography images reveals dental implant stability. *Int J Oral Maxillofac Surg* 2021; 50: 1609-16.
24. Kitagawa Y, Ohga N, Asaka T, Sato J, Hata H, Helman J, et al. Imaging modalities for drug-related osteonecrosis of the jaw (3), positron emission tomography imaging for the diagnosis of medication-related osteonecrosis of the jaw. *Jpn Dent Sci Rev* 2019; 55: 65-70.
25. Chappard D, Guggenbuhl P, Legrand E, Baslé MF, Audran M. Texture analysis of X-ray radiographs is correlated with bone histomorphometry. *J Bone Miner Metab* 2005; 23: 24-9.